Electron-microscopy study of the triple-q to single-q phase transition in the incommensurate phase of quartz under stress

E. Snoeck and C. Roucau
CEMES-LOE, Boîte Postale 4347, 31055 Toulouse CEDEX, France
(Received 17 September 1991)

The triple-**q** to single-**q** phase transition in quartz has been studied by electron microscopy using a heating straining device, stress being applied along the x axis. The interpretation of the experimental images obtained for small values of stress is in agreement with theoretical predictions. The presence of an intermediate state between the triple-**q** and single-**q** modulated phases has been observed for higher values of stress. It can be described as a double-**q** state where the two wave vectors are tilted from the **y** direction by an angle of $+\varphi$ and $-\varphi$ that decreases to 0 in the single-**q** stripe phase.

I. INTRODUCTION

The existence of the incommensurate phase in quartz observed at the α-β phase transition[1-3] has been successfully explained by Aslanyan and Levanyuk[4,5] using the Landau theory of phase transitions and considering a coupling of elastic strains with the gradient of the order parameter of the α-β phase transition. The minimization of the free energy deduced from their model allows stabilization of either the single-**q** or the triple-**q** modulated phase. In the case of a triple-**q** modulation, the modulation star must be composed of three equal length vectors q_i at 120° from each other and tilted by an angle $\pm\varphi$ from the **y** directions. In the single-**q** state, the wave vector should be parallel to **y**. In the absence of any external field, the triple-**q** state is the most stable, as evidenced by different experiments in real space[2,3,7,8] and in reciprocal space.[6,9-11]

Recently, Dolino *et al.* have shown that a uniaxial stress applied in the *ab* plane can induce a transition from the triple-**q** to the single-**q** state.[12] Vallade and Petit have then studied the possible evolution of the modulation wave vectors of the triple-**q** phase under stress.[13] An increase of the applied stress would change both the length and the orientation of triple-**q** wave vectors to a single wave vector parallel to the **y** direction. The sequence of phase transitions with increasing temperature at a given applied stress different from zero would be α, triple-**q** incommensurate, single-**q** incommensurate, β [experiments also show that the 1-**q** state exists without any applied stress in a small range of temperature around T_i (Ref. 14) but it has not been observed by electron microscopy].

As already shown, electron microscopy is quite relevant for the study of phase transitions in quartz.[2,3,7,8] We therefore used a heating straining sample holder to perform experiments on the appearance of the strip phase. In this paper we report on previous work on the triple-**q** modulated phase and then investigate the transition from this triple-**q** state to the single one by applying *in situ* a stress along the **x** direction.

II. EXPERIMENT

The experiments are performed in a Jeol 200CX electron microscope operating at 200 kV. A simple tilt-straining device realized in our laboratory is employed. It only permits us to stretch the sample ($\sigma < 0$) and includes a heating resistor. The temperature can vary between 300 and 1300 K without any contamination or oxidation.

The quartz single crystal is cut perpendicular to the **c** axis into $8\times2\times0.2$ mm^3 thin plates. Two holes are drilled at the extremity to allow for stress application. Samples are then thinned using ion milling until a central hole is achieved. They are then covered with a thin layer of amorphous carbon to avoid electrostatic charging. Radiation damage was minimized by observing the samples at temperatures close to the α-β transition (around 850 K).

The temperature is stabilized by controlling the electrical current in the heating resistor. The stress is applied at high temperature when the sample is in the triple-**q** incommensurate phase but it cannot be quantitatively measured. Coujou *et al.* have determined the spatial distribution of strains around hole in such samples.[15] In agreement with their results, we studied the two more highly stressed regions perpendicular to the direction of stress on either side of the central hole.

III. RESULTS

A. Triple-q phase

Figure 1 shows the incommensurate phase observed by electron microscopy without applied stress. The image was obtained by using the 110 reflection in the (a^*,b^*) plane, which contains the three wave vectors. The contrast observed on such micrographs is consistent with a triple-**q** incommensurate phase and their interpretation has already been discussed in Ref. 8. Here we only report the main results.

Because of a thermal gradient at the sample surface, a

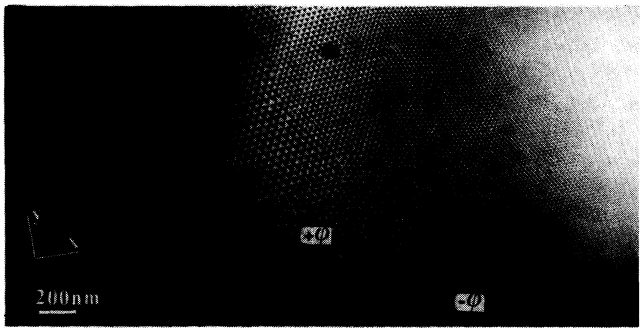

FIG. 1. Dark field image of the incommensurate phase of quartz obtained using a 110 reflection and its six satellites.

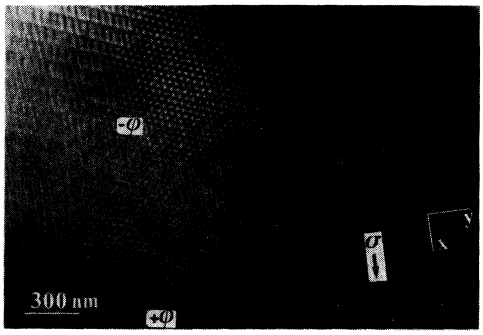

FIG. 2. Dark field image of the stressed incommensurate phase of quartz. A uniaxial stress applied along **x** induced a triple-**q** to single-**q** phase transition.

large domain of existence of the incommensurate phase can be observed between the α phase (left-hand side of the micrograph) and the β phase (right-hand side). The triangular dark-light contrast patterns may be interpreted as the result from an interference contrast between the main Bragg reflection and the six satellite spots that surround it at the $\pm q_i$ value ($i=1,2,3$).[8] As predicted by the theory of Aslanyan *et al.*, these three q_i wave vectors are tilted from the **y** directions by an angle φ depending on the temperature. Then the two equivalent values $+\varphi$ and $-\varphi$ induce the presence of the "$\pm\varphi$ macrodomains" structure that is clearly visible in Fig. 1. The observed interfaces between these macrodomains support the theoretical investigations of Walker[16] and Saint-Gregoire.[17] The different sizes of the equilateral black and white triangles correspond to the different values of the wave vectors depending on temperature. The highly blurred contrast near T_i (in the vicinity of the β phase) does not allow us to confirm the presence of a single-**q** state under zero stress at this temperature. All the characteristics of this triple-**q** phase deduced from this electron micrograph are consistent with the results obtained from x-ray,[6,9] neutron,[10] or γ (Ref. 11) diffraction. In addition, the elongated triangular textures observed at T_c between the α phase and the incommensurate one, which has not been observed by other experimental methods, may constitute an intermediate phase that is planned to be discussed elsewhere.

B. Evidence of the triple-q–single-q phase transition

Figure 2 depicts an electron micrograph observed on a quartz sample under uniaxial stress. It has been achieved using the 110 diffraction spot in the [001] zone axis. As in Fig. 1, a large domain of the incommensurate phase is visible. Stress direction is reported in the figure and slightly deviates from the **x** direction. On the right-hand side of the micrograph, fringes parallel to the **x** direction can be observed. They exhibit a periodicity of 20 nm and correspond to the single-**q** strip phase with a wave vector parallel to the [100] direction. The contrasts at the center of the figure are quite different from the equilateral triangle images observed on the triple-**q** phase in Fig. 1. Nevertheless, the 120° angle between the three directions of the modulation indicates the triple-**q** state. Another element supporting the assumption that we are observing an image of the triple-**q** incommensurate phase is the presence of the two "$\pm\varphi$ macrodomains" visible in the center of this micrograph. As already mentioned these domains are only allowed on the triple-**q** state when it is not on the single-**q** state. As predicted by Vallade's theory[13] discussed in the next section, the triple-**q** state is altered by stress and the contrasts change as noted in this figure.

Another important feature of this micrograph can be observed on the elongated triangular structure near T_c (left-hand side of the image) that seems more regular than those observed without applied stress. Even if it is fairly obvious that stress does influence the different phases (α, β, triple-**q**, single-**q**), the effect on this "intermediate phase" is not well understood and will only be discussed after further experiments.

C. Behavior of the triple-q incommensurate phase under stress

Our interpretation of the equilateral triangle dark-light contrast obtained by electron microscopy using an $hk0$ reflection has already been reported in Ref. 8. In this model we considered an interference between the main reflection $hk0$ and the six satellites that surround it at the hexagonal positions: $+\mathbf{q}_i$, $-\mathbf{q}_i$ (i.e. $\mathbf{q}_i,\mathbf{q}_j$ at 120° and $\|\mathbf{q}_i\|=\|\mathbf{q}_j\|$). Figure 3(a) shows six satellites tilted at an angle $+\varphi$ from the **y** directions (at the $\pm q_i$ positions) and six others tilted at an angle $-\varphi$ (at the $\pm q_i'$ positions). Considering equal amplitudes $a_q=a(\pm q_i)$ and equal phases ϕ_{+i},ϕ_{-i} for all satellites and an amplitude a_0 and phase ϕ_0 for the $hk0$ basic spot, the interference between those reflections will produce an image intensity that can be written in the form of Eq. (3) of Ref. 8:

$$I(\mathbf{r})=4a_0a_q\sum_i\cos[(\phi_{+i}+\phi_{-i})/2-\phi_0]\times\cos[\mathbf{q}_i\cdot\mathbf{r}+(\phi_{+i}-\phi_{-i})/2]+\text{const}\ . \quad (1)$$

An image computed with this equation is given in Fig. 3(b) (considering one system of six satellites only: i.e., one φ macrodomain) and is in agreement with the regular equilateral triangles contrast of Fig. 1.

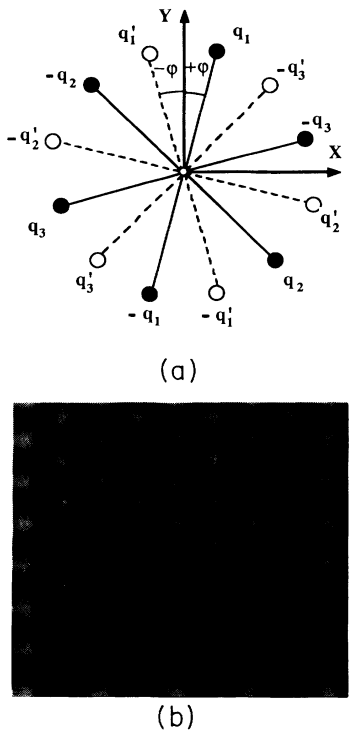

FIG. 3. (a) Schematic representation of satellite peak positions at $\pm q_i$ deviated at an angle $+\varphi$ (solid circles) and $-\varphi$ (open circles) from the **y** directions. (b) Calculated image corresponding to the model of Eq. (1) using the six satellites at the $\pm q_i$ positions (see text).

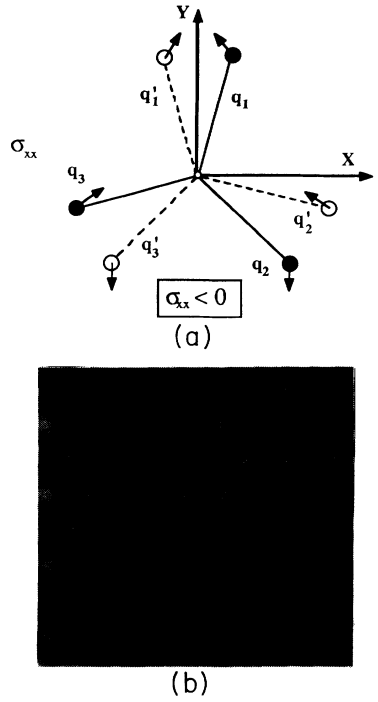

FIG. 4. (a) Schematic representation proposed by Vallade and Petit (Fig. 1 of Ref. 13) of the stress-induced changes of the modulation wave vectors in the triple-**q** state of quartz. (b) Calculated image with six satellites of *one* macrodomain in the positions proposed in (a).

To account for the contrasts observed in the center of Fig. 2, changes occurring in the wave vectors of the triple-**q** phase have to be envisaged. Then consider the model proposed by Vallade *et al.*[13] about the influence of stress on the wave vectors of the triple-**q** incommensurate phase. Applying a phenomenological theory in the small-stress limit, they propose changes to the length and orientation of the three wave vectors under stress. Figure 4(a) schematically depicts the displacements proposed for an external stress $\sigma' < 0$ along **x** (Fig. 1 of Ref. 13). For clarity we have only reported the positive values $(+q_i, +q_i')$ of the wave vectors. We have computed the contrast obtained from the interference between these six satellites at $+q_{i,} - q_i$ displaced in agreement with the model proposed, and the main $hk0$ reflection. We have then imposed the small changes they propose for the wave-vector lengths and orientations at the three vectors $\mathbf{q}_i$ with the constraint $\sum_i \mathbf{q}_i = \mathbf{0}$. In a first approximation, equal amplitudes $a_q = a(\pm q_i)$ were chosen for the six satellite reflections. A calculated image using these parameters in Eq. (1) is presented in Fig. 4(b). It is consistent with the experimental one of Fig. 2. Moreover, Vallade's model assumes that the σ' component of stress is not expected to completely delete the degeneracy of the $\pm\varphi$ sign and therefore does not affect the presence of $\pm\varphi$ macrodomains. This is in agreement with our electron microscopy observations on the presence of $\pm\varphi$ macrodomains (clearly visible in Fig. 2). These observations confirm the predictive assumptions of Vallade and Petit about the effects of small stress on the triple-**q** state in the incommensurate phase of quartz.

If the applied stress on the sample is increased, the triple-**q** phase evolves to the single-**q** one and the associated contrasts change to those presented in Fig. 5. On the right size of this micrograph, a regular single-**q** state of 20-nm periodicity is visible. On the left size, the contrast is not so periodic and consists of a elongated and distorted triangle texture. To explain these contrasts, consider our experimental conditions where stress is ap-

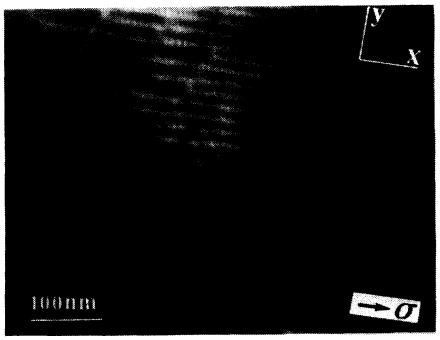

FIG. 5. Dark field image observed on the stressed incommensurate phase of quartz (see text).

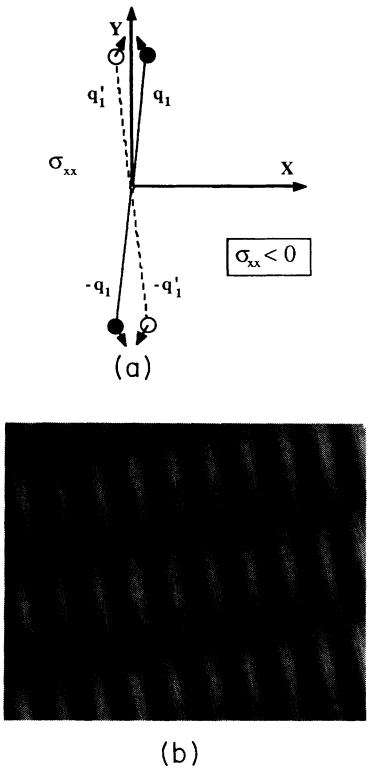

FIG. 6. (a) Schematic representation of persistent wave vectors for an important stress along **x** (b) Calculated images using the four satellites presented in (a).

plied along **x** and suppose that this stress favors only the wave vectors perpendicular to the stress direction. Two modulation wave vectors could be obtained: that is, those disoriented from the **y** direction of the angles $+\varphi$ and $-\varphi$. These vectors belong to the two different macrodomains of the triple-**q** phase. By increasing stress they will tilt and blend into one vector in the exact **y** direction, perpendicular to the stress, to achieve the single-**q** incommensurate modulation (that would be different for a stress applied along one of the **y** directions which would favor two single-**q** phases[12,13]). Suppose that the contrast observed on the micrograph in Fig. 5. are also due to an interference phenomena between the main $hk0$ spot and the satellites that surround it (as we considered in previous states). Figure 6(a) shows the supposed wave vectors. We have then to calculate the image intensity considering the interference between the main reflection $hk0$ and the four satellites that surround it in positions: $+q_1$, $-q_1$, $+q_1'$, and $-q_1'$ with q_1 and $-q_1'$ at 2φ each from the other (for the calculated images we have chose $2\varphi=20°$). We have also assumed that there is no preferred direction between q_1 and q_1' [i.e., we have taken $\|q_1\|=\|q_1'\|$ and equal amplitudes for the satellites: $a(\pm q_1)=a(\pm q_1')$]. We have also refined the agreement between our experimental images and those calculated by considering the interference between the two satellites (q_1 and q_1') with a weight three times less. The intensity would be

$$I(\mathbf{r})=I_0\{\cos[\mathbf{q}_1\cdot\mathbf{r}+(\phi_{+1}-\phi_{-1})/2] + \cos[\mathbf{q}_1'\cdot\mathbf{r}+(\phi'_{+1}-\phi'_{-1})/2]\} + (I_0/3)\cos[(\mathbf{q}_1+\mathbf{q}_1')\cdot\mathbf{r}+(\phi_{+1}-\phi'_{-1})]+\text{const}\ . \quad (2)$$

A simulated image following Eq. (2) is presented in Fig. 6(b) and has to be compared to that of Fig. 5.

The agreement between our micrographs and the calculated images seems to confirm our assumption on the use of these two wave vectors belonging to different $+\varphi$ and $-\varphi$ domains to pass from the triple-**q** phase to the single one. The use of such (q_i,q_i') wave vectors has already been proposed in Ref. 7 to explain an intermediate state observed around T_c between the α phase and the triple-**q** one in the incommensurate phases of quartz and of $AlPO_4$.[7,18]

In brief, small stress applied along the **x** direction first induces changes in the orientation, length, and intensity of the three wave vectors as predicted by Vallade [Fig. 4(a)]. These changes favor the vectors perpendicular to the direction of stress while the amplitude of the other wave vectors vanishes. Because of the two possible values $\pm\varphi$ of the angle between the wave vector and the **y** direction, two wave vectors stand out [Fig. 5(b)]. They achieve a "double-**q**" intermediate phase built from two wave vectors of different macrodomains. Increasing the stress will induce a decrease of the φ angle to 0 that stabilizes a single-**q** state with a wave vector parallel to the **y** direction.

IV. CONCLUSION

The phase transition in quartz from the triple-**q** incommensurate state to the single-**q** state under uniaxial stress has been observed in real space. The interpretation of the contrasts observed for different values of stress agree with the theoretical assumptions proposed by Vallade and Petit in the small-stress limits. For higher applied stress, elongated and distorted triangle patterns are observed. This contrast could be explained by assuming that modulation consists there of two wave vectors q_i and q_i' deviated of an angle $+\varphi$ and $-\varphi$, respectively, from the **y** direction. This angle decreases to zero in the single-**q** state. The assumption of a possible "double-**q**" intermediate state should be confirmed by diffraction experiments. Further electron microscopy studies are needed to understand the influence of stress applied along other directions (particularly along the **y** axis where two single-**q** stripe phases should be favored).

ACKNOWLEDGMENTS

We are grateful to Dr. A. Couret and Dr. D. Caillard for helping us in the *in situ* applied stress experiments and P. Sopena for preparing TEM samples. We also want to thank Dr. M. Vallade for fruitful and highly motivating discussions. The CEMES-LOE is Unité Propre No. 8011 du CNRS.

[1]J. P. Bacheimer and G. Dolino, Phys. Rev. B **11**, 3195 (1975).
[2]G. Van Tendeloo, J. Van Landuyt, and S. Amelinckx, Phys. Status Solidi A **33**, 723 (1976).
[3]J. Van Landuyt, G. Van Tendeloo, S. Amelinckx, and M. B. Walker, Phys. Rev.B **31**, 2986 (1985).
[4]T. A. Aslanyan and A. P. Levanyuk, Solid State Commun. **31**, 547 (1979).
[5]T. A. Aslanyan, A. P. Levanyuk, M. Vallade, and J. Lajzerowicz, J. Phys. C. **16**, 6505 (1983).
[6]N. Kato and K. Gouhara, Phys. Rev. B **34**, 2001 (1986).
[7]E. Snoeck, C. Roucau, and P. Saint-Gregoire, J. Phys. **47**, 2041 (1986).
[8]E. Snoeck, C. Roucau, and H. Mutka, J. Phys. **50**, 937 (1989).
[9]K. Gouhara and N. Kato, J. Phys. Soc. Jpn. **53**, 1869 (1985).
[10]G. Dolino, J. P. Bacheimer, B. Berge, and C. M. E. Zeyen, J. Phys. **45**, 361 (1984).
[11]P. Bastie and G. Dolino, Phys. Rev. B **31**, 2857 (1985).
[12]G. Dolino, P. Bastie, B. Berge, M. Vallade, J. Bethke, L. P. Regnault, and C. M. E. Zeyen, Europhys. Lett. **3**, 601 (1987).
[13]M. Vallade and M. Petit, Phys. Status Solidi A **111**, 155 (1989).
[14]P. Bastie, F. Mogeon, and C. M. E. Zeyen, Phys. Rev. B **38**, 786 (1988).
[15]A. Coujou, Ph. Lours, N. A. Roy, D. Caillard, and N. Clement, Acta Metall. Mater. **32**, 825 (1990).
[16]M. B. Walker, Phys. Rev. B **28**, 6407 (1983).
[17]P. Saint-Gregoire, V. Janovec, E. Snoeck, C. Roucau, and Z. Zikmund (to be published).
[18]E. Snoeck, C. Roucau, P. Saint-Grégoire, and E. Philippot, Ferroelectrics **79**, (1988).

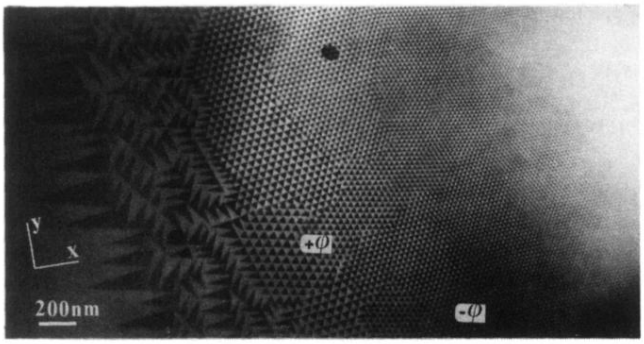

FIG. 1. Dark field image of the incommensurate phase of quartz obtained using a 110 reflection and its six satellites.

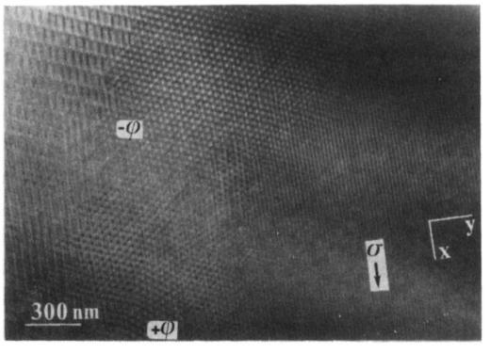

FIG. 2. Dark field image of the stressed incommensurate phase of quartz. A uniaxial stress applied along **x** induced a triple-**q** to single-**q** phase transition.

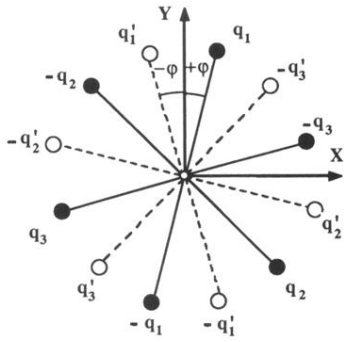

(a)

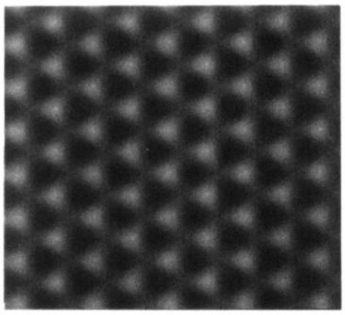

(b)

FIG. 3. (a) Schematic representation of satellite peak positions at $\pm q_i$ deviated at an angle $+\varphi$ (solid circles) and $-\varphi$ (open circles) from the **y** directions. (b) Calculated image corresponding to the model of Eq. (1) using the six satellites at the $\pm q_i$ positions (see text).

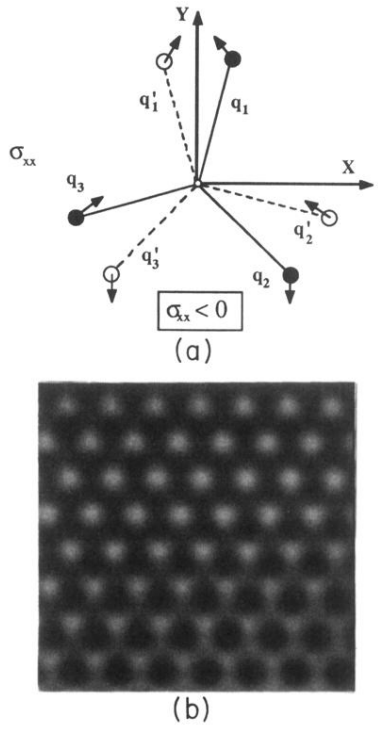

FIG. 4. (a) Schematic representation proposed by Vallade and Petit (Fig. 1 of Ref. 13) of the stress-induced changes of the modulation wave vectors in the triple-**q** state of quartz. (b) Calculated image with six satellites of *one* macrodomain in the positions proposed in (a).

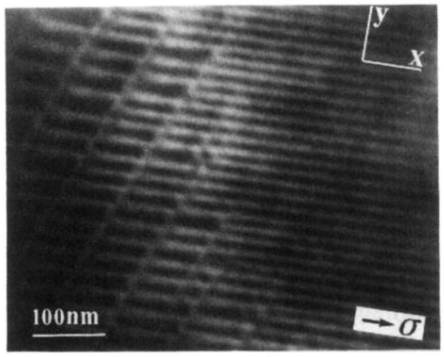

FIG. 5. Dark field image observed on the stressed incommensurate phase of quartz (see text).

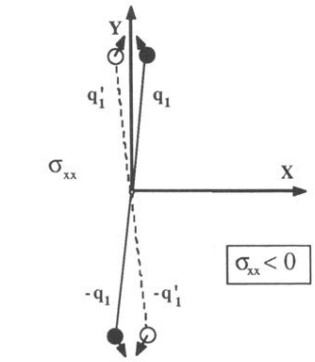

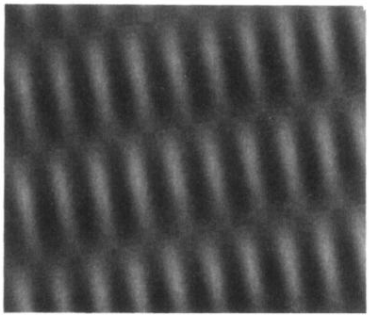

(b)

FIG. 6. (a) Schematic representation of persistent wave vectors for an important stress along **x** (b) Calculated images using the four satellites presented in (a).